Discrete and 1D Co(II) Coordination Compounds with Bridging Imidazole-Functionalized Terpy

Emilie Delahaye, Marie Noelle Lalloz-vogel, Carine Duhayon, Jean-pascal Sutter

EurJIC
European Journal of Inorganic Chemistry

Research Article
doi.org/10.1002/ejic.202500048

Chemistry Europe
European Chemical Societies Publishing

www.eurjic.org

Discrete and 1D Co(II) Coordination Compounds with Bridging Imidazole-Functionalized Terpy

Emilie Delahaye,* Marie Noelle Lalloz-Vogel, Carine Duhayon, and Jean-Pascal Sutter*

Solvothermal conditions enable the formation of polynuclear Co(II) compounds with 4′-[*p*-(Imidazol-1-yl)phenyl]-2,2′:6′,2″-terpyridine (L) acting as a bridging ligand. 1D coordination polymer $[Co_2(L)_2(Cl)_4].5H_2O$, **1**, and discrete $[Co_2(L)(Cl)_4(DMF)]_2$, **2**, can be selectively obtained by tuning the $CoCl_2$/L ratio involved in the reaction. A peculiar feature in complex **2** is the occurrence of tetrahedral and octahedral Co centers bridged by a chloride atom, whereas Co(II) is six-coordinated in **1**. The crystal structures of both compounds have been characterized by single-crystal X-ray diffraction studies. Magnetic studies have evidenced a canted antiferromagnetic (i.e., weak ferromagnet) behavior for **2**.

1. Introduction

Terpy, *i.e.*, 2, 2′:6′, 2″-terpyridine is an ubiquitous ligand in coordination chemistry of transition metal and lanthanide metal ions.[1,2] It has been widely involved in the design of compounds for optical, magnetic, catalytic, and biological properties.[3–11] In addition to the benefits of tridentate coordination ensuring for stable complexes, the interest in this ligand also lies in the possibility of functionalizing it with a wide range of chemical groups, to modulate its electronic characteristics or introduce auxiliary properties.[1,12,13] The anchoring of a π-conjugated substituent in the 4′-position is suitable for propagating the electronic effect between the chemical function at the periphery and the metal connected to Terpy.[14] When this group can act as a ligand, the π-conjugation may also mediate magnetic interaction between metal centers bridge by the functionalized terpy.[5]

In this context, we have investigated the particular case of a Terpy ligand substituted in 4′-position by a *p*-(imidazole-1-yl)-phenyl unit[15] (L hereafter) as possible ligand for bridging two metal centers. To date, this ligand has mainly shown a propensity to form mononuclear complexes by the coordination of the terpy unit to the metal center.[2,16] We report here that solvothermal conditions enable formation of polynuclear compounds with L acting as a bridging ligand linked by its terpyridine and imidazole moieties to metal ions.

Interestingly, the dimensionality of the compounds could be tuned by varying the L/M(II) salt ratio, yielding either the 1D coordination polymer $[Co_2(L)_2(Cl)_4].5H_2O$, **1**, or the discrete tetranuclear complex, $[Co_2(L)(Cl)_4(DMF)]_2$, **2**. A peculiar feature in **2** is the occurrence of tetrahedral and octahedral Co centers bridged by a chloride atom, whereas Co(II) is six-coordinated in **1**. Magnetic studies have evidenced a canted antiferromagnet behavior (*i.e.*, weak ferromagnet) for **2**.

2. Results and Discussion

2.1. Syntheses

The preparation of 4′-[*p*-(Imidazol-1-yl)phenyl]-2,2′:6′,2″-terpyridine, L, was reported in a two-step procedure.[15] We have now developed a one-step synthesis from *p*-(1H-imidazol-1-yl)benzaldehyde and 2-acetylpyridine that affords L in about 56% yield.

The reaction of L with $CoCl_2$ in DMF was performed under identical solvothermal conditions for **1** and **2**; the reaction product is determined by the initial Co(II)/L ratio. When the reaction was carried out with a 1/1 ratio of reactants, a coordination polymer of formula $[Co_2(L)_2(Cl)_4].5H_2O$, **1**, was obtained. Increasing the Co(II) ratio led to the formation of a discrete tetranuclear complex with two Co(II) ions per L, $[Co_2(L)(Cl)_4(DMF)]_2$, **2**. The latter was obtained as the only product for a Co/L ratio of 4.

2.2. Crystal Structures

$[Co_2(L)_2(Cl)_4].5H_2O$, **1**, crystallizes in the triclinic space group *P*-1 (**Table 1**) and consists in a 1D coordination polymer (**Figure 1** and Figure S2a, Supporting Information). The asymmetric unit contains two independent molecular moieties, each consisting of one Co(II) ion, one L ligand, and two Cl^- anions, as well as five solvate water molecules. The Co1 and Co2 are hexacoordinated with four nitrogen atoms, three from a terpyridine moiety and

E. Delahaye, C. Duhayon, J.-P. Sutter
Laboratoire de Chimie de Coordination du CNRS (LCC-CNRS)
Université de Toulouse, CNRS
31077 Toulouse, France
E-mail: emilie.delahaye@lcc-toulouse.fr
jean-pascal.sutter@lcc-toulouse.fr

M. N. Lalloz-Vogel
Institut de Physique et Chimie des Matériaux de Strasbourg
Université de Strasbourg, CNRS UMR 7504
67034 Strasbourg, France

Supporting information for this article is available on the WWW under https://doi.org/10.1002/ejic.202500048

Research Article
doi.org/10.1002/ejic.202500048

Table 1. Crystallographic data for compounds 1 and 2.

	1	2
Empirical formula	$C_{48}H_{44}Cl_4Co_2N_{10}O_5$	$C_{54}H_{48}Cl_8Co_4N_{12}O_2$
Molecular weight (g mol^{-1})	1100.62	1416.41
Crystal system	Triclinic	Triclinic
Space group	*P*-1	*P*-1
Crystal size (mm^3)	0.03 × 0.07 × 0.22	0.12 × 0.14 × 0.14
Unit cell		
a (Å)	10.8112(1)	8.448(2)
b (Å)	11.6456(2)	8.871(2)
c (Å)	20.2301(2)	19.993(5)
α (°)	81.807(1)	89.105(8)
β (°)	83.088(1)	79.133(8)
γ (°)	81.270(1)	80.438(8)
V (Å^3)	2479.11(6)	1450.8(6)
Z	2	1
T (K)	100	100
D_{calc}	1.47	1.62
μ (mm^{-1})	7.693 (CuKα)	1.55 (MoKα)
Refl. collected	86 631	47 320
Independent refl.	10 555	7267
R_{int}	0.0459	0.0442
Nb parameters	649	361
Refl. with $I > 2\sigma(I)$	8945	6821
S	0.98	0.98
R1 [$I > 2\sigma(I)$]	0.0640	0.029
wR2 [$I > 2\sigma(I)$]	0.2044	0.0767
Residual electron density (ë.Å − 3)	−0.76/2.31	−0.72/1.64
CCDC reference	2 388 226	2 388 225

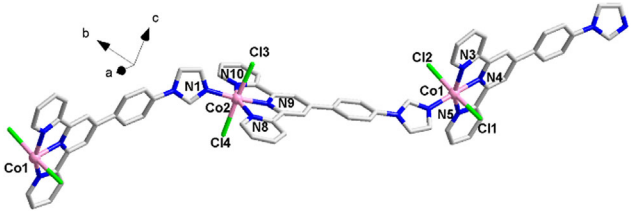

Figure 1. 1D polymeric structure in compound **1** (Co in pink, Cl in green, C in gray, N in blue, H, and solvents are omitted for clarity). Selected bond distances (Å): Co1-Cl1, 2.5172(11); Co1-Cl2, 2.5470(11); Co1-N3, 2.133(4); Co1-N4, 2.063(3); Co1-N5, 2.153(4); Co1-N6, 2.075(3); Co2-Cl3, 2.4859(10); Co2-Cl4, 2.4839(10); Co2-N1, 2.084(3); Co2-N8, 2.133(3); Co2-N9, 2.058(3); Co2-N10, 2.165(3).

one from an imidazole group, and two chloride anions bonded to the metal atom. The shape of the coordination polyhedra of the Co centers was assessed by Continuous Shape Measures[17] performed with SHAPE,[18] and found to correspond to distorted octahedral geometries (Shape values in Table S1, Supporting Information). Each L ligand is linked to two Co(II) ions, and each Co(II) coordinates to two L by the means of a terpy and an imidazole unit, thus developing a 1D coordination polymer.

The crystal packing reveals obvious π–π stacking between the aromatic groups of the ligands (*i.e.*, pyridyl and phenyl units) of adjacent chains. It reveals also H-bonds between chloride atoms and solvate water molecules or between the water molecules themselves. The distance between Co centers of adjacent chains is quite large with 7.856(1) Å and 7.5671(7) Å (for Co1···Co1$_{1-x,2-y,-z}$ and Co1···Co1$_{1-x,-y,1-z}$, respectively).

$[Co_2(L)(Cl)_4(DMF)]_2$, **2**, crystallizes in the triclinic space group *P*-1 (Table 1). Its asymmetric unit contains a molecular fragment consisting in one L ligand linked to two Co^{2+} ions with four Cl^- anions, and one DMF molecule in their coordination spheres. The molecular structure (**Figure 2** and Figure S2b, Supporting Information) consists in two such moieties in a head-to-tail arrangement with a chloride atom bridging two Co(II) ions. The coordination sphere of Co1 accommodates six atoms consisting in three nitrogen atoms of the terpyridine moiety, two chloride atoms, and one oxygen atom from DMF. The Co2 displays a tetra-coordinated environment made of three chloride anions and one nitrogen atom from the imidazole moiety. The shape of the coordination polyhedra of the two Co centers correspond respectively to distorted octahedral and tetrahedral geometries (Shape values in Table S1, Supporting Information). The molecular complex results from the assembly of two $[Co_2(L)(Cl)_4(DMF)]$ fragments by means of a bridging chloride atom (Cl2) linking each tetrahedral Co to the octahedral Co of the partner fragment. The length of the Co—Cl bonds (see Figure 2) suggests that a $[CoCl_3]^-$ moiety acts as a ligand for a $[Co(Terpy)(DMF)Cl]^+$ unit. The Co1-Cl2-Co2 angle is equal to 116° and the shortest intramolecular Co···Co distance is 4.14 Å. A selection of bond distances is given in the figures captions.

The crystal packing reveals several intramolecular H-bonds established between the Cl-atoms and hydrogen atoms of the pyridyl and imidazolyl units of L of neighboring complexes (Figure S3a, Supporting Information). These H-bond interactions interconnect the Co moieties in a 2D network (Figure S3b, Supporting Information). Such short contacts are meaningful with respect to the intermolecular magnetic interactions observed for **2** (see below).

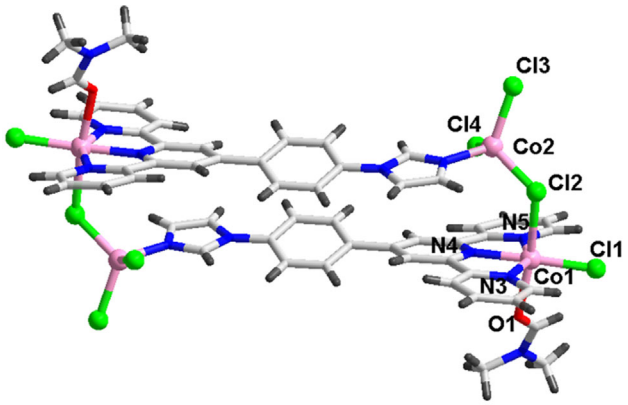

Figure 2. Tetranuclear complex contained in compound **2** (Co in blue and pink, Cl in green, C in gray, N in blue and O in red, H in black). Selected bond lengths (Å): Co1-Cl1, 2.2997(7); Co1-Cl2, 2.6163(7); Co1-O1, 2.180(1); Co2-Cl2, 2.2699(7); Co2-Cl3, 2.2524(6) Å; Co2-Cl4, 2.2441(6).

Research Article
doi.org/10.1002/ejic.202500048

Thermal analysis and Lebail refinements for **1** and **2** confirm the formulation and the phase purity of the isolated microcrystalline products (Figure S4 and S5, Supporting Information). The UV–visible spectra show the expected absorption bands for octahedral Co^{2+} ion in **1** and **2**, and, for the latter, bands characteristic for Co^{2+} ion in tetrahedral environment are also found (Figure S6, Supporting Information).

2.3. Magnetic Properties

The temperature dependence of the molar magnetic susceptibility, χ_M, for **1** and **2** has been collected between 300 and 2 K; results are plotted as $\chi_M T$ product for a $[Co(L)(Cl)_2].2.5H_2O$ unit and $[Co_2(L)(Cl)_4(DMF)]_2$, respectively. For **1**, the value of $\chi_M T$ obtained at 300 K is 2.81 $cm^3\ mol^{-1}\ K$, in agreement with the usual values for high-spin Co(II).[19] This value is steadily reduced as T is lowered and reaches 1.62 $cm^3\ mol^{-1}\ K$ for 2 K (**Figure 3**). This behavior and the value found at 2 K suggest the absence of exchange interaction between the Co centers within the chain. This is not surprising given the length of the organic moiety linking the metal centers. The steady decrease observed between 200 and 2 K can be attributed to the intrinsic behavior of the Co(II), that is the effect of zero-field splitting (ZFS). This conclusion is supported by the field dependence of the magnetization (Figure 3, insert). At 2 K, the magnetization shows an increase for fields up to 30 kOe and tends to level off at around 2 μ_B for larger fields (2.02 μ_B are reached for 50 kOe). This value is lower that the magnetization at saturation expected for a $S = 3/2$ but is characteristic for Co(II) with substantial magnetic anisotropy.[20]

These behaviors have been analyzed by considering an $S = 3/2$ spin with ZFS. The modeling of $\chi_M T = f(T)$ was carried out taking into account the axial parameter D of the ZFS and a possible exchange interaction, which was considered within the mean field approximation (*i.e.*, zJ). A very good agreement (Figure 3) was obtained for $D = 83 \pm 1\ cm^{-1}$, $zJ = -0.048 \pm 0.006\ cm^{-1}$, and $g = 2.486 \pm 0.002$. The very low value for zJ confirms the lack of magnetic interactions between the Co centers, and the large D supports substantial magnetic anisotropy. More accurate characterization for the latter was obtained from the analyses of the $M = f(H)$ behaviors at different temperatures between 2 and 5 K; for these modeling the axial and rhombic, E, ZFS parameters have been refined. Best fits led to $D = 61 \pm 6\ cm^{-1}$, $E = 13.9 \pm 0.6\ cm^{-1}$, and $g = 2.373 \pm 0.004$. The value of D reveals a rather large magnetic anisotropy with, however, a substantial rhombic component ($E/D = 0.22$), a situation likely arising from the strongly distorted coordination geometry. The positive sign for D indicates planar anisotropy, that is often found for Co(II) in distorted octahedral coordination sphere.[20,21]

The $\chi_M T = f(T)$ for **2** is shown in **Figure 4**. At 300 K, the value for $\chi_M T$ is 11.0 $cm^3\ mol^{-1}\ K$, which corresponds to 2.75 $cm^3\ mol^{-1}\ K$ per Co(II) with $S = 3/2$ and $g = 2.4$, in agreement with usual values for this ion in tetrahedral and octahedral coordination spheres.[20–22] When lowering the temperature, $\chi_M T$ initially decreases slightly, and below 100 K, the decrease is more pronounced before showing a trend reversal at around 12 K. This low T behavior was found to be strongly field dependent. With $H = 1000$ Oe (Figure 4 and Figure S7a, Supporting Information), $\chi_M T$ reaches 4.8 $cm^3\ mol^{-1}\ K$ for 12 K and slightly increases to 5.0 for 8 K before dropping rapidly for low T. With $H = 25$ Oe (Figure 4 and Figure S7b, Supporting Information), after the minimum at 12 K, the increase of $\chi_M T$ is stronger and reaches 9.4 $cm^3\ mol^{-1}\ K$ for 6 K, before dropping to 5.1 for 2 K.

The variation of $\chi_M T$ between 300 and 12 K can be interpreted as the contribution of ZFS and a weak antiferromagnetic interaction between the two Co ions bridged by a chlorine atom. The latter is rationalized by the super-exchange that leads to an overlap of the π-type magnetic orbitals of the tetrahedral Co(II), d_{xy}, d_{xz}, and d_{zy}, with the σ-type magnetic orbitals $d_{x^2-y^2}$ and d_{z^2} of the hexacoordinated Co(II) via the lone pairs of the bridging Cl atom. And this antiferromagnetic interaction is anticipated to be weak due to the long Co1-Cl2 bond (2.6163(7) Å), which should considerably reduce the orbital overlap. The magnetic behavior for

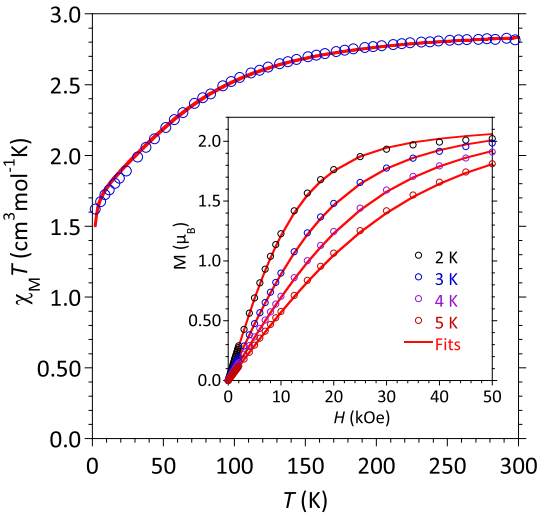

Figure 3. Experimental (O) and calculated (—) $\chi_M T = f(T)$ and (*insert*) $M = f(H)$ behaviors for **1**.

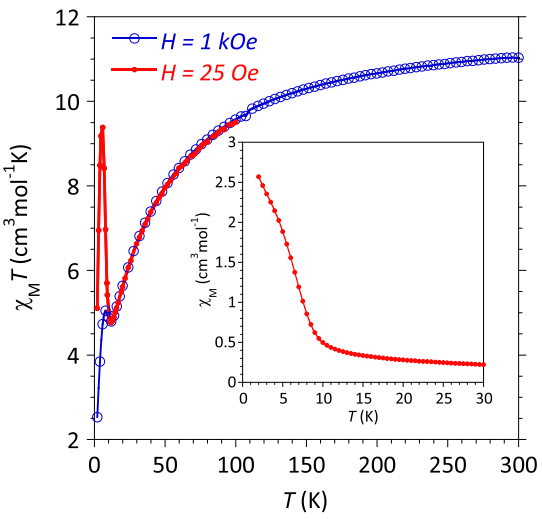

Figure 4. $\chi_M T = f(T)$ and (*insert*) $\chi_M = f(T)$ behaviors for **1** recorded in a field of 25 Oe (in red) and 1 kOe (in blue).

Research Article
doi.org/10.1002/ejic.202500048

1 allows to exclude any exchange interaction between the Co-dimers mediated by the L-bridging ligand. However, the behavior below 12 K reveals some additional contribution no longer of molecular origin but reminiscent of a canted antiferromagnetic system (*i.e.*, a weak ferromagnet).[23] The $\chi_M = f(T)$ recorded with $H = 25$ Oe exhibits a steep raise below 10 K (insert Figure 4) that is characteristic for a ferromagnetic correlation, and possibly magnetic ordering. This is supported by the Curie–Weiss plots (Figure S7c,d, Supporting Information) and the appearance of an out-of-phase component in AC susceptibility, χ_M'', which however is no longer observed with an applied static field (**Figure 5** and Figure S7e, Supporting Information).[24] The maximum of the $\chi_M'' = f(T)$ traces is frequency dependent (5.3 and 6.3 K, respectively, for 1 and 1488 Hz) and the temperature dependence of the relaxation time derived from these data follows an Arrhenius behavior (Figure S7f, Supporting Information) characterized by an energy barrier $U = 241$ K and $\tau_0 = 1.8 \times 10^{-21}$ s. The very low value of τ_0 rules out the possibility that a low dimensional anisotropic spin system (*i.e.*, a single molecule magnet) is responsible for this behavior, it can most likely be ascribed to motion of domain walls.[24]

The field dependence of the magnetization between 2 and 5 K (Figure S7g, Supporting Information) exhibits a very gradual increase with field and does not saturate (4 μ_B are obtained for 50 kOe at 2 K). Interestingly, a small spontaneous magnetization (for $H = 0$) is observed at 2, 3, and 4 K, which is reduced with T and vanishes for 5 K (Figure S7h, Supporting Information). Such a feature is typical for a canted antiferromagnetic systems.[25]

All these observations suggest the occurrence of a long-range magnetic correlation between the Co centers resulting in a behavior reminiscent of a canted antiferromagnetic system. The H-bonds between the chlorine atoms and hydrogen atoms of the pyridyl and imidazole moieties (see discussion on the crystal structure) are the most likely pathway for magnetic interactions between the molecules. This results in 2D networks of interconnected $[Co_2Cl_4]$ units, and antiferromagnetic interactions between them are highly likely. But due to the strong magnetic anisotropy of the tetra- and the hexa-coordinated Co(II) centers, spin canting can result, leading to the observed behavior characteristic for a weak ferromagnet. Possibility to replace chlorine atoms by bromo or iodo atoms to evaluate effect on magnetic behavior has been explored without success.

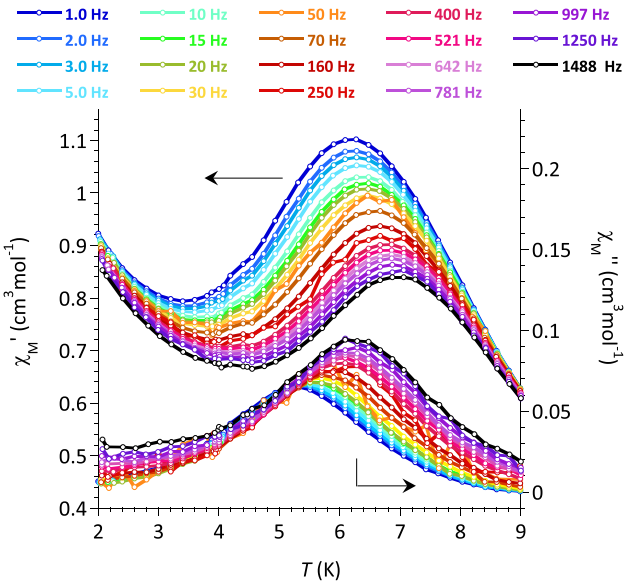

Figure 5. AC susceptibility for **2** in zero field: temperature dependence for χ_M' and χ_M'' for different frequencies ($H_{AC} = 3$ Oe).

3. Conclusion

Until now, the 4′-[*p*-(Imidazol-1-yl)phenyl]-2,2′:6′,2″-terpyridine ligand (L) was known to lead to complexes with only the terpyridine group coordinated to the metal centers. This was illustrated in several reactions with Co^{2+}, Ni^{2+} or Zn^{2+} ions in a 1/1 ratio, yielding $[M(\mathbf{L})_2]^{2+}$ or $[M(\mathbf{L})]^{2+}$ complexes where imidazole remained systematically uncoordinated.[16] All these reactions were performed in ambient conditions. The results reported here show that solvothermal synthesis enable the formation of complexes with L acting as a bridging ligand.

The rationale behind this observation certainly lies in the increased solubility of intermediate species for higher temperatures, including mononuclear compounds where only Terpy entities are bound, and their dissociation under these synthesis conditions. This equilibrium of species in solution makes it possible to reach the ultimate product in which L coordinates via its Terpy and imidazole sites, despite the greater binding strength of the former.

Interestingly, in same solvothermal conditions, the modulation of $CoCl_2$/L ratio allow access to different products, as illustrated by 1D coordination polymer $[Co_2(L)_2(Cl)_4].5H_2O$, **1**, and discrete $[Co_2(L)(Cl)_4(DMF)]_2$, **2**, achieved in this study. These observations most likely apply to other potentially bridging Terpy-derived ligands, which would considerably broaden the scope of such ligands.

4. Experimental Section

Materials and Methods

Reagents and solvents were from commercial sources and were used as received. Elemental analyses are carried out with a Perkin–Elmer 2400 series II instrument. FT-IR spectra were collected on a Perkin–Elmer Frontier spectrometer. TGA-TDA experiments were performed using a Mettler Toledo TGA/DSC 3$^+$ STAR^e System (heating rates of 5 °C min^{-1} under air stream). UV–visible studies were performed in solid state (samples were diluted in KBr) with a Perkin–Elmer LAMBDA 950 spectrometer (spectra recorded in reflection mode, using an integrating sphere, with a resolution of 4 nm). NMR spectra in solution were recorded using a Bruker AVANCE 300 (300 MHz) spectrometer.

Syntheses: 4′-[*p*-(Imidazol-1-yl)phenyl]-2,2′:6′,2″-terpyridine, L[15]

KOH (3.35 g, 60 mmol) is dissolved at room temperature in 150 mL of ethanol (absolute 99.9%). After complete dissolution, 28–30% aqueous ammonia (75 mL, 2 mol) is added, followed, after 15 min, by 4-(1H-imidazol-1-yl)benzaldehyde (5.00 g, 30 mmol) and 2-acetylpyridine

(7.20 g, 60 mmol). The mixture is stirred for 72 h at room temperature, gradually turning khaki green and forming a precipitate. The thin powder is filtered and washed with a cooled water/ethanol solution (1/1 vv, 20 mL) and then with ether (V = 30 mL) before being recrystallized in ethanol to yield L (m = 7 g, Y = 58%) as a white crystalline powder. Analytical data (below) are in agreement with those reported earlier for 4′-[*p*-(Imidazol-1-yl)phenyl]-2,2′:6′,2″-terpyridine.

Elemental analysis for $C_{24}H_{17}N_5$ ($M = 375$ g mol^{-1}): Found (Calc.) (%): C 76.51 (76.80), H 4.33 (4.53), N 18.53 (18.67). ^{1}H NMR ($CDCl_3$): δ (ppm) = 8.75 (d, J = 3.1 Hz, 3), 8,72 (m, 2), 8.65 (dt, J = 8.0, J = 1.2 Hz, 2), 7.97 (m, 2), 7.93 (d, J = 3.1 Hz, 1), 7.87 (tt, J = 7.7, J = 1.6 Hz, 2), 7.49 (dt, J = 8.8 Hz, J = 2.2 Hz, 2), 7.35 (m, 3), 7.24 (d, J = 1.6 Hz, 1). ^{13}C NMR ($CDCl_3$): δ (ppm) = 156.15, 156.00, 149.17, 148.72, 137.79, 137.67, 136.98, 135.50, 130.67, 128.87, 124.02, 122.12, 121.41, 118.60, 118.08. Infrared (reflectance, cm^{-1}, Figure S1, Supporting Information): 3123 (w), 3097 (w), 3058 (w), 3008 (w), 1611 (m), 1601 (m), 1583 (s), 1565 (m), 1549 (w), 1526 (s), 1489 (w), 1466 (s), 1440 (w), 1421 (w), 1386 (m), 1312 (m), 1246 (m), 1194 (w), 1115 (m), 1093 (w), 1064 (s), 1038 (m), 988 (m), 961 (m), 905 (m), 884 (w), 849 (w), 828 (s), 788 (s), 740 (m), 731 (s), 658 (s), 614 (m), 575 (w), 528 (s), 464 (m), 412 (m).

Syntheses: $[Co_2(L)_2(Cl)_4].5H_2O$, 1

L (37.5 mg, 0.1 mmol) and $CoCl_2.6H_2O$ (23.8 mg, 0.1 mmol) are introduced in a 20 mL glass vial, and DMF (6 mL) is added. The vial is closed with a screw-cap and heated at 95 °C (heating ramp of 30 min) for 24 h. After cooling to room temperature (cooling ramp of 3 h), the solid is isolated by filtration and washed with diethyl ether, yielding **1** (m = 70 mg, Y = 64%) as a reddish crystalline powder.

Elemental analysis for $C_{48}H_{44}Cl_4Co_2N_{10}O_5$ ($M = 1100$ g mol^{-1}): Found (Calc.) (%): C 52.56 (52.36), H 3.62 (4.00), N 12.74 (12.73). Infrared (reflectance, cm^{-1}, Figure S1, Supporting Information): 3490 (m), 3383 (m), 3168 (vw), 3152 (w), 3127 (w), 3102 (w), 3069 (w), 1609 (s), 1601 (s), 1554 (w), 1534 (s), 1474 (s), 1435 (m), 1408 (s), 1309 (m), 1249 (m), 1161 (w), 1101 (w), 1054 (s), 1016 (s), 965 (s), 937 (m), 898 (m), 841 (s), 789 (s), 745 (m), 731 (s), 673 (w), 658 (s), 640 (m), 528 (s), 502 (w), 413 (s).

Syntheses: $[Co_2(L)(Cl)_4(DMF)]_2$, 2

Same procedure as for **1** but with 0.4 mmol (95.2 mg) of $CoCl_2.6H_2O$. Compound **2** (50 mg, Y = 70%) is isolated as bluish-green crystals.

Elemental analysis for $C_{54}H_{48}Cl_8Co_4N_{12}O_2$ ($M = 1416$ g mol^{-1}): Found (Calc.) (%): C 45.40 (45.76), H 3.02 (3.39), N 11.53 (11.86). Infrared (reflectance, cm^{-1}, Figure S1, Supporting Information): 3413 (m), 3143 (w), 3121 (w), 3060 (w), 2926 (vw), 1653 (m), 1602 (s), 1569 (w), 1553 (w), 1533 (s), 1505 (w), 1475 (s), 1436 (m), 1411 (s), 1374 (w), 1310 (w), 1248 (m), 1161 (w), 1134 (w), 1109 (w), 1061 (m), 1025 (m), 1016 (m), 965 (m), 903 (w), 831 (s), 792 (s), 753 (m), 734 (m), 672 (m), 658 (s), 643 (s), 621 (w), 581 (w), 517 (s), 418 (s).

Crystallography

Single crystals suitable for X-ray diffraction (XRD) are coated with paratone oil. The X-ray crystallographic data are obtained from a Rigaku XtaLAB Synergy-S diffractometer (Cu Kα radiation source, compound 1) or from a Bruker Apex2 diffractometer (Mo Kα radiation source, compound 2). An Oxford Cryosystem is used for low-temperature measurements. The structures have been solved by direct methods using ShelXT[26] or Superflip[27] and refined by means of least-square procedures on F^2 using the program CRYSTALS.[28] The scattering factors for all the atoms are used as listed in the International Tables for X-Ray Crystallography.[29] Absorption correction is performed using a multi-scan procedure. All nonhydrogen atoms are refined anisotropically. The H atoms are usually located in a difference map except some on solvate molecules (compound 1), but those attached to carbon atoms are systematically repositioned geometrically. The H atoms are initially refined with soft restraints on the bond lengths and angles to regularize their geometry and Uiso(H) (in the range 1.2–1.5 times Ueq of the parent atom), after which the positions are refined with riding constraints. The CCDC numbers are 2 388 226 for **1**, 2 388 225 for **2**.

Powder XRD (PXRD) patterns were collected with a Miniflex 600 (Rigaku, $\theta/2\theta$ mode, and HPAD linear detector) operating under Cu Kα radiation. Phase purity for each compound was confirmed by Lebail refinement on the experimental PXRD patterns using the Fullprof software.[30] For each iteration, all parameters (lattice parameters: a, b, c, α, β, γ; halfwidth parameters: U, V, W and shape parameters: eta, X) were refined until reaching convergence.

Magnetic Measurements

Magnetic measurements were carried out with a Quantum Design MPMS 5S SQUID magnetometer in the temperature range 2–300 K. The measurements were performed on polycrystalline samples mixed with grease and put in gelatin capsules. The temperature dependences of the magnetization were measured in an applied field of 1 kOe (or as specified in, the text) and the isothermal field dependence of the magnetizations was collected up to 5 T at temperatures between 2 and 5 K. The molar susceptibility (χ_M) was corrected for sample holder, grease and for the diamagnetic contribution of all the atoms by using Pascal's tables.[19] AC susceptibility has been collected in the frequency range 1–1500 Hz. Assessment of the exchange interactions and/or ZFS parameters have been done considering an S = 3/2 spin for Co(II), the software PHI[31] was used for fitting the $\chi_M T = f(T)$ and $M = f(H)$ behaviors.

Acknowledgements

The authors are grateful to M. J.-F. Meunier (LCC) for technical assistance in the magnetic data collections, to M. B. Martin (LCC) for technical assistance in ATD/ATG measurements, and to Mrs I. Borget (LCC) for performing the elemental analyses.

Conflict of Interest

The authors declare no conflict of interest.

Data Availability Statement

The data that support the findings of this study are available from the corresponding author upon reasonable request.

Keywords: cobalt ion · coordination polymers · imidazole · terpyridine

[1] S. F. Kainat, M. B. Hawsawi, E. U. Mughal, N. Naeem, A. M. Almohyawi, H. M. Altass, E. M. Hussein, A. Sadiq, Z. Moussa, A. S. Abd-El-Aziz, S. A. Ahmed, *RSC Adv.* **2024**, *14*, 21464.

[2] X. Yu, Y. Hu, C. Guo, Z. Chen, H. Wang, X. Li, *Supramol. Mater.* **2022**, *1*, 100017.
[3] O. Stefanczyk, G. Li, K. Kumar, Q. Song, K. Nakabayashi, S. Ohkoshi, *Eur. J. Inorg. Chem.*, *37*, e202400353.
[4] Y. Zhou, X.-Q. Wei, Y. Gu, Q.-Q. Zhao, D. Shao, *Eur. J. Inorg. Chem.* **2023**, *26*, e202200666.
[5] A. Winter, U. S. Schubert, *ChemCatChem* **2020**, *12*, 2890.
[6] N. Busto, M. C. Carrión, S. Montanaro, B. D. de Greñu, T. Biver, F. A. Jalón, B. R. Manzano, B. García, *Dalton Trans.* **2020**, *49*, 13372.
[7] T. Mandal, V. Singh, J. Choudhury, *Chem. Asian J.* **2019**, *14*, 4774.
[8] M. Nakaya, R. Ohtani, J. W. Shin, M. Nakamura, L. F. Lindoy, S. Hayami, *Dalton Trans.* **2018**, *47*, 13809.
[9] J. Lhoste, A. Pérez-Campos, N. Henry, T. Loiseau, P. Rabu, F. Abraham, *Dalton Trans.* **2011**, *40*, 9136.
[10] S. Hayami, Y. Komatsu, T. Shimizu, H. Kamihata, Y. H. Lee, *Coord. Chem. Rev.* **2011**, *255*, 1981.
[11] E. C. Constable, *Chem. Soc. Rev.* **2007**, *36*, 246.
[12] J. Husson, M. Knorr, *J. Heterocycl. Chem.* **2012**, *49*, 453.
[13] M. Heller, U. S. Schubert, *Eur. J. Org. Chem.* **2003**, *2003*, 947.
[14] E. U. Mughal, M. Mirzaei, A. Sadiq, S. Fatima, A. Naseem, N. Naeem, N. Fatima, S. Kausar, A. A. Altaf, M. N. Zafar, B. A. Khan, *R. Soc. Open Sci.* **2020**, *7*, 201208.
[15] C. X. Wang, L. Li, W. T. Yu, J. X. Yang, J. Y. Wu, *Acta Crystallogr., Sect. E:Struct. Rep. Online* **2006**, *62*, o246.
[16] W. W. Fu, Q. Huang, S. T. Liu, W. J. Wu, J. R. Shen, S. H. Li, *Russ. J. Coord. Chem.* **2017**, *43*, 670.
[17] S. Alvarez, P. Alemany, D. Casanova, J. Cirera, M. Llunell, D. Avnir, *Coord. Chem. Rev.* **2005**, *249*, 1693.
[18] M. Llunell, D. Casanova, J. Cirera, P. Alemany, S. Alvarez, *SHAPE: Program for the Stereochemical Analysis of Molecular Fragments by Means of Continuous Shape Measures and Associated Tools*, University of Barcelona, Barcelona **2013**.
[19] O. Kahn, *Molecular Magnetism*, Wiley-VCH, Weinheim **1993**.
[20] J. Titiš, R. Boča, *Inorg. Chem.* **2011**, *50*, 11838.
[21] A. K. Bar, C. Pichon, J.-P. Sutter, *Coord. Chem. Rev.* **2016**, *308*, 346.
[22] Y. Rechkemmer, F. D. Breitgoff, M. van der Meer, M. Atanasov, M. Hakl, M. Orlita, P. Neugebauer, F. Neese, B. Sarkar, J. van Slageren, *Nat. Commun.* **2016**, *7*, 10467.
[23] D.-F. Weng, Z.-M. Wang, S. Gao, *Chem. Soc. Rev.* **2011**, *40*, 3157.
[24] H. A. Groenendijk, A. J. van Duyneveldt, R. D. Willett, *Phys. BC* **1980**, *101*, 320.
[25] B. Koteswararao, T. Chakrabarty, T. Basu, B. K. Hazra, P. V. Srinivasarao, P. L. Paulose, S. Srinath, *Sci. Rep.* **2017**, *7*, 8300.
[26] G. M. Sheldrick, *Acta Crystallogr., Sect. A:Found. Adv.* **2015**, *71*, 3.
[27] L. Palatinus, G. Chapuis, *J. Appl. Crystallogr.* **2007**, *40*, 786.
[28] P. W. Betteridge, J. R. Carruthers, R. I. Cooper, K. Prout, D. J. Watkin, *J. Appl. Crystallogr.* **2003**, *36*, 1487.
[29] A. J. C. Wilson, V. Geist, *Cryst. Res. Technol.* **1993**, *28*, 110.
[30] J. Rodriguez-Carvajal, *Phys. B Condens. Matter* **1993**, *192*, 55.
[31] N. F. Chilton, R. P. Anderson, L. D. Turner, A. Soncini, K. S. Murray, *J. Comput. Chem.* **2013**, *34*, 1164.

Manuscript received: January 27, 2025
Revised manuscript received: April 8, 2025
Version of record online: